Eur. Phys. J. C 4, 533–541 (1998)
DOI 10.1007/s100529800794

THE EUROPEAN PHYSICAL JOURNAL C

On the possibility of the dual Meissner effect induced by instantons

Kurt Langfeld

Institut für Theoretische Physik, Universität Tübingen, D-72076 Tübingen, Germany

Received: 5 September 1997 / Published online: 23 February 1998

Abstract. The classical Yang-Mills equation of motion is numerically investigated in the Lorentz gauge for a SU(2) gauge group. The color-electric field of two point-like charges is studied in the "empty" vacuum and in a state with an instanton present. The major effect for a fixed orientation of the instanton is that the color-electric field lines are expelled or attracted from the instanton region depending on the orientation of the instanton. If over the orientations of the instanton is averaged, this effect drops out. In this case of a random instanton orientation, we find that the external color-electric field is expelled from the instanton core. The origin of this effect is discussed.

1 Introduction

One of the most challenging problems in hadron physics nowadays is to understand the confinement of quarks in quantum-chromodynamics (QCD), which is the theory of strong interactions. From large scale numerical investigations of lattice Yang-Mills theory [1,2], we know that QCD yields confinement, since Wilson's area law is satisfied. This implies that a linear rising confinement potential is formed between static color sources. Unfortunately, the numerical efforts have not yet revealed the basic mechanism of confinement. The knowledge of the qualitative mechanism would help to construct effective hadron theories the predictive power of which is not limited by unphysical quark thresholds [3]. Only effective quark models which heuristically incorporate the confinement are so far available. I would like to mention the Global Color Models [4] which realize confinement either by avoiding the pole at the real axis of the quark propagator or by infrared slavery. In [5] it was proposed that quark confinement is due to random quark interactions induced by random gluonic background fields.

A promising idea to understand the feature of quark confinement from first principles was given by 't Hooft and Mandelstam. They propose that the so-called Abelian gauges are suited to understand the basic mechanism of confinement which is obscured in other gauges [6]. In these Abelian gauges magnetic monopoles emerge because of a residual U(1) gauge degree of freedom which is unfixed [7]. If these monopoles condense due to the Yang-Mills dynamics, a dual Meissner effect takes place implying that the color-electric flux is expelled from the vacuum. This scenario would naturally explain the linear rising potential between sources of color-electric flux. Subsequently, heuristic models were developed which explore the formation of an color-electric flux tube [8]. However, the dynamics which leads to the condensation of the monopoles is not understood so far.

The original idea of 't Hooft and Mandelstam has gained further support by a recent success [9] of Seiberg and Witten. They showed that the monopoles of $N = 2$ (non-confining) super-symmetric Yang-Mills theory start to condense, if the theory is explicitly broken down to $N = 1$ (confining) SUSY. One should, however, keep in mind that this scenario in super-symmetric Yang-Mills theory is quite different from that in standard QCD. Whereas in the previous case magnetic monopoles are present in the particle spectrum, magnetic monopoles are induced by gauge transformations in the latter case.

The quasi-particles of standard Yang-Mills theory which show up as a solution of the classical Yang-Mills equation of motion are instantons [10]. An implicit scheme to construct all instanton solutions was provided in [11]. Novel explicit instanton configurations for a SU(N), $N \geq 3$ can be found in [12]. Instantons are generally believed to play an important role in the QCD ground state. They may possibly trigger the spontaneous breaking of chiral symmetry [13] and offer an explanation of the $U_A(1)$ problem [14].

Numerical investigations, based on a classical instanton interaction, show that instantons are strongly correlated in the Yang-Mills ground state implying that they occur as a liquid [15] rather than in a dilute gas phase [16]. Including quantum fluctuations, it was discovered that instantons possess a medium range attractive interaction which is solely due to the instability of the perturbative vacuum [17]. The strong-coupling expansion within the field strength approach to Yang-Mills theory [18] suggests that the interaction due to quantum effects is strong enough to induce a condensation of instantons [19]. Whether the instantons exist in a crystal type structure or in a

strongly correlated liquid is still beyond the scope of the present approaches.

The question whether instantons are important for the dual Meissner effect has gained recent attention [20–24]. In order to address this question, the profile of an instanton in Abelian gauges were investigated in continuum Yang-Mills theory [20,21] as well as in the lattice version [22, 23]. In [20], a monopole world line was observed which penetrates the center of the instanton. In contrast, the lattice simulations [22,23] have reported closed loops of monopoles which encircle the center of the instanton. The length of the monopole loop was investigated throughout the deconfinement transition. The discrepancy between the lattice and the continuum approach was clarified by Brower at al. [21]. They showed that the configurations which minimize the gauge fixing functional indeed lead to closed monopole world lines. The conclusion at hand is that large monopole loops play an important role for confinement. Recently, lattice calculations reported an enhanced probability for monopoles inside the instanton [24] indicating that instantons play a role in the context of the dual Meissner effect.

In this paper, we will directly focus on this role of the instantons. For this purpose, we will numerically solve the SU(2) Yang-Mills equation of motion with two static color sources present. The color-electric flux stemming from the color sources will be investigated in the "empty" vacuum and in a vacuum where an instanton is present. Whether the external color-electric field lines are expelled or attracted depends on the orientation of the instanton relative to the charges. If over the orientation of the instanton is averaged, the picture changes qualitatively. We will provide evidence that in the latter case the external field is repulsed from the instanton core.

The paper is organized as follows: in the following section, we briefly review some aspects concerning the relation of instantons and confinement. In Sect. 3, the Meissner effect in solid state physics is addressed for a later comparison with the situation in SU(2) Yang-Mills theory. The numerical approach to solve the classical Yang-Mills equation of motion is introduced in Sect. 4. It is shown that this approach nicely reproduces an instanton configuration. In Subsect. 4.3, two point-like color-electric charges are added. The electric field lines stemming from these charges are investigated in an "empty" vacuum (Subsect. 4.3) and in a state with an instanton present (Subsect. 4.4). The case of a random instanton orientation is presented in Sect. 5. Conclusions as well as an argument to understand qualitatively the numerical results of the latter section are left to the final section.

2 Instantons imply confinement?

In this section, we briefly review some results in the literature which address the question how relevant instantons are for the confinement mechanism.

This question has a long history [25–27]. A semi-classical evaluation of the Yang-Mills partition function by Aharonov et al. [25] has indicated that instantons support the existence of infinite long flux tubes (fluxon). These strings with non-vanishing flux appear as fluctuations on top of the instanton background. It was shown that an ensemble of these random-walking "fluxons" gives rise to Wilson's area law. In this scenario, the impact of the instantons on confinement is secondary.

Considering fluctuations around an instanton, 't Hooft showed that large size instantons receive a large weight in the Yang-Mills partition function [14]. Expectation values of condensates are even ill-defined due to the contribution of these large size instantons. Subsequently, it was argued by Shuryak that the presence of quarks and gluons cure the large size instanton problem [26]. He showed that the presence of a non-vanishing quark and/or gluon density provides a natural cutoff on the instanton radius. As a consequence, the presence of quarks and gluons yield an increase in the vacuum energy density implying that they should be expelled from an instanton dominated vacuum. This picture naturally supports the MIT bag model of hadronic matter. Note that we will focus at the classical level when we will elaborate below the response of the instantons on the external charges.

In their pioneering work, Polikarpov and Veselov provided evidence that the instantons play a minor role for confinement [27]. They studied the emergence of instantons in SU(2) lattice Yang-Mills theory, when a equilibrium lattice configuration is cooled down. They extracted the ratio χ of the string tension of the configuration *after* cooling with the one of the lattice equilibrium configuration as function of the topological charge present on the lattice. One crucial observation is that χ increases with increasing topological charge Q. For instance, χ reaches 20% for a sufficiently large Wilson loop and for $Q = 3$. However, large topological charges rarely appear on the lattice. The value of χ averaged over the instanton vacua which appear by freezing out equilibrium configurations is of order 5%.

The outcome of the latter considerations is twofold: an instanton medium which emerges from the freezing of a lattice equilibrium configuration cannot give rise to the full string tension. Fluctuations on top of the instanton medium seem to play an important role for confinement. Recent lattice simulations indicate that these fluctuations might be magnetic strings, which are attached to the instanton [24]. Secondly, lattice equilibrium configurations are dominated by fluctuations rather than by the classical solutions of the Yang-Mills equation of motion. The later fact is confirmed by recent studies in [23]. The authors investigated the evolution of the topological charge Q during the cooling process. They found that the lattice equilibrium configurations are dominated by configurations with $Q = 0$. However, if these configurations are cooled down, configurations with larger Q-values emerge. This demonstrates that the fluctuations on the lattice (at realistic values of the coupling strength) are large enough to change the topological charge Q.

In this paper, we will elaborate a detailed picture of the response of an instanton to the presence of static charges on a "microscopic" level. We will thereby provide new in-

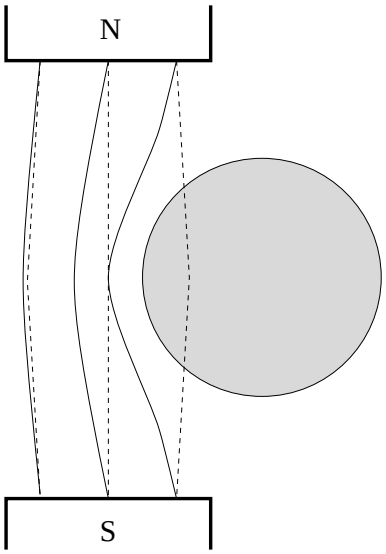

Fig. 1. The Meissner effect: magnetic field lines with a superconducting cylinder present (*solid lines*) and without the cylinder (*dashed lines*)

formation to clarify the role of the instantons for the dual Meissner effect rather than to estimate the importance of the (semi-) classical vacuum for the true ground state of Yang-Mills theory.

3 The Meissner effect of solid state physics

In 1933 Meissner and Ochsenfeld discovered that superconductors expel magnetic flux. The microscopic ingredient which leads to this effect is the condensation of electric charge, which is carried by pairs of electrons [29]. For later comparison with the Yang-Mills case, we briefly review this effect by considering a Landau-Ginzburg theory [30] which is described in terms of the Lagrangian

$$\mathcal{L} = |(\partial_\mu + i\mathcal{A}_\mu(x))\,\phi(x)|^2 + \frac{1}{4e^2}\mathcal{F}_{\mu\nu}^2 - j_\mu(x)\mathcal{A}_\mu(x) + V(\phi^2)\,, \qquad (1)$$

where $\mathcal{F}_{\mu\nu}$ is the electro-magnetic field strength built from the gauge potential $\mathcal{A}_\mu$, and e is the electric charge. $V(\phi^2)$ is the tree-level Higgs-potential, which is minimal for a non-vanishing value $\phi^2 = \phi_0^2$ providing a condensation of the scalar field. $j_\mu(x)$ is the external current. The Lagrangian is invariant under U(1) gauge transformations. The scalar field $\phi(x)$ transforms homogeneously under these transformations and therefore carries electric charge.

In order to mimic the scenario of a super-conductor, we assume that the scalar field forms a homogeneous condensate ϕ_0 of electric charge, which breaks the U(1) gauge symmetry. The classical equation of motion can be easily obtained from (1), i.e.

$$\partial_\mu \mathcal{F}_{\mu\nu}(x) \;-\; 2e^2\phi_0^2\,\mathcal{A}_\nu(x) \;=\; -j_\nu(x)\,. \qquad (2)$$

In the gauge $\partial_\mu \mathcal{A}_\mu(x) = 0$, this equation can be transformed into an Helmholtz equation for the magnetic field $\mathcal{B}_i$. In the absence of external currents, this equation becomes

$$\partial^2 \mathcal{B}_i(x) \;-\; 2e^2\phi_0^2\,\mathcal{B}_i(x) \;=\; 0\,. \qquad (3)$$

This is the key equation to understand the Meissner effect. Equation (3) tells us that the magnetic field exponentially decreases inside a super-conductor with slope given by the strength of the condensate ϕ_0. Figure 1 qualitatively shows the behavior of the magnetic field lines, if a superconducting cylinder is present. The main observation is that the magnetic field lines are expelled from the superconducting region.

Let us compare London's equation (2) with the classical equation of motion of an SU(2) Yang-Mills theory. This equation can be derived from the Euclidean action which is defined in the appendix, i.e.

$$\partial_\mu F^a_{\mu\nu}[A](x) \;-\; \epsilon^{abc} F^c_{\nu\mu}[A]\,A^b_\mu(x) \;=\; -g^2\,j^a_\nu(x)\,, \qquad (4)$$

where ϵ^{abc} is the anti-symmetric tensor in 3 dimensions, and $j^a_\nu(x)$ are the external currents. The field strength, i.e.

$$F^a_{\mu\nu}[A] \;=\; \partial_\mu A^a_\nu \;-\; \partial_\nu A^a_\mu \;+\; \epsilon^{abc} A^b_\mu A^c_\nu\,, \qquad (5)$$

is constructed from the non-Abelian gauge field $A^a_\mu(x)$. The external source j^a_μ is a real function of space-time and can be understood as the current generated by Euclidean quark fields (see (23)). We will adopt the Lorentz gauge, $\partial_\mu A^a_\mu(x) = 0$, and will study the impact of this current on instantons throughout this paper.

For a vanishing external current ($j^a_\nu = 0$), (4) allows for non-trivial solutions, which are known as instantons [10]. In the gauge $\partial_\mu A^a_\mu(x) = 0$, their gauge field and the corresponding field strength is given by

$$A^{a\,inst}_\mu(x) = \eta^a_{\mu\nu} x_\nu \,\frac{2}{x^2+\rho^2}\,,$$
$$F^{a\,inst}_{\mu\nu}(x) = -\,\eta^a_{\mu\nu}\,\frac{4\rho^2}{(x^2+\rho^2)^2}\,, \qquad (6)$$

where $\eta^a_{\mu\nu}$ are the anti-symmetric 't Hooft symbols, i.e.

$$\eta^a_{0i} \;=\; \delta_{ai}\,, \qquad \eta^a_{ik} \;=\; \epsilon^{aik}\,, \quad i,k = 1\ldots 3\,, \qquad (7)$$

and ρ is the radius of the instanton. Instantons therefore correspond to spots of non-vanishing field strength.

Let us now briefly discuss the linear response of the gauge field, i.e. $a^a_\mu(x)$, to the external source $j^a_\nu(x)$. Decomposing $A^a_\mu(x) = A^{a\,inst}_\mu(x) + a^a_\mu(x)$, we assume that the current is sufficiently weak implying that one can expand the e.o.m. (4) to linear order in $a^a_\mu(x)$. If we confine us to the region close to the center of the instanton, i.e. $\sqrt{x^2} \ll \rho$, the e.o.m. becomes

$$\partial^2 a^a_\nu(x) - \frac{3}{2}\epsilon^{abc} F^c_{\nu\mu}\left[A^{inst}(x=0)\right]\,a^b_\mu(x) = -g^2\,j^a_\nu(x);\,. \qquad (8)$$

Since the matrix $\epsilon^{abc}F^c_{\mu\nu}$ possesses negative eigenvalues, (8) describes screening of the field strength as well as

anti-screening depending on the color index a under consideration. The field strength $F^a_{\mu\nu}$ at the instanton center sets the scale of the (anti-) screening length and therefore plays a similar role as the scalar field ϕ_0^2 in (2). We learn from (8) that Meissner type effects occur due to the non-linear nature of the Yang-Mills e.o.m., if instantons are present in the ground state of SU(2) Yang-Mills theory. The crucial difference is, however, that these effects lead to a repulsion or an attraction of the color-electric field lines depending on the orientation of the instanton.

In this paper, we will further investigate these effects resorting to numerical methods in order to go beyond the linear response theory. We will provide evidence that the electric flux produced by the charges is expelled from the instanton core, if we average over the instanton orientation. In this case, the above leading order effect obtained by the linear response approach drops out.

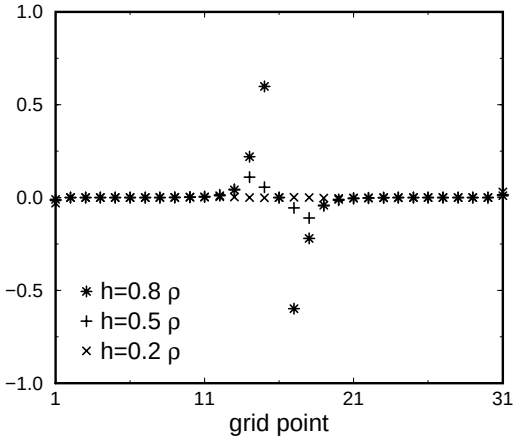

Fig. 2. The "0" produced from the discretized version of the e.o.m. (4) by inserting the instanton configuration (6)

4 The dual Meissner effect of SU(2) Yang-Mills theory

4.1 The numerical approach

In the following, we will work in the Lorentz gauge

$$\partial_\mu A^a_\mu(x) \;=\; 0\,. \tag{9}$$

We will numerically investigate the solutions of the classical equation of motion (4) (we set $g^2 = 1$ for simplicity) of SU(2) Yang-Mills theory, which is a non-linear second order partial differential equation. To this aim, we discretize the 4-dimensional Euclidean space-time on a grid consisting of 31^4 points, and replace derivatives by the corresponding differences, e.g.

$$\partial_\mu f(x) \to \frac{1}{2h}(f(x+h\hat{e}_\mu) \,-\, f(x-h\hat{e}_\mu))\,, \tag{10}$$

where $\hat{e}_\mu$ is the unit vector in μ-direction, and where h is the grid spacing. The discretized partial differential equation is then solved by iteration. For definiteness, we have chosen Neumann boundary conditions. We have checked that the impact of the boundaries on the field configurations under consideration is small (see below).

The approach should not be confused with the lattice version of Yang-Mills theory [1]. The grid is only a mathematical tool to solve the partial differential equation. For our purposes, we need not worry about local gauge invariance, but confine ourself to the definite gauge choice (9).

In order to get a first idea of the error due to the discretization (and to check the set up of the program), we cast the analytically known instanton configuration $A^{a\,inst}_\mu(x)$ (6) onto the grid, and checked to what extent the discretized version of the l.h.s. of (4) reproduces the zero at the r.h.s. (note that the external source j^a_μ is set to zero at the moment). Choosing $x_{2,3,4} = 0$ (this selects a line which passes the center of the instanton) and e.g. $a = 2$ and $\nu = 3$, the deviation from zero is shown in Fig. 2 as function of x_1 for several values of the grid spacing h. The result should be compared with the intrinsic scale which is set by the maximum field strength of the instanton (4 in units of the instanton radius). The most important observation is that the result becomes significantly better, if h is decreased. This confirms that the discretization works correctly.

4.2 The instanton on the grid

In this subsection, we study the grid version of an instanton configuration, which emerges as a solution of the discretized e.o.m. (4) at zero external source ($j^a_\mu(x) = 0$). The SU(2) instanton possesses eight zero-modes, since the instanton configuration breaks symmetries of the Lagrangian. Four translational, three rotational and one dilatational degrees of freedom do not lead to a change of the action. In the pseudo-particle description of the instanton, these zero-modes give rise to collective coordinates, which must be fixed in order to arrive at a definite configuration. For this purpose, it is convenient to employ a procedure which minimizes the action by the method of steepest decent. Then zero-modes do not contribute to the gradient configuration which is added in each iteration step to the actual profile in order to further reduce the action. This implies that the starting configuration of the iteration process completely fixes the collective coordinates of the instanton. Here we have chosen the analytic profile (6) as the starting configuration.

After convergence was obtained, we have calculated the color-electric field of our grid configuration with the help of a discretized version of the field strength tensor (5). Choosing the color direction $a = 1$, we learn from (6) and (7) that the only non-vanishing color-electric field points in $\hat{e}_1$ direction. We then have compared the numerical result for the space-time dependence of this color-electric field, i.e. $E^1_1(x)$, with the analytic form (6). The result in shown in Fig. 3. For $h = 0.5\,\rho$, the field strength in the center of the instanton is somewhat underestimated, whereas the result is satisfactory for $h = 0.2\,\rho$. However, the influ-

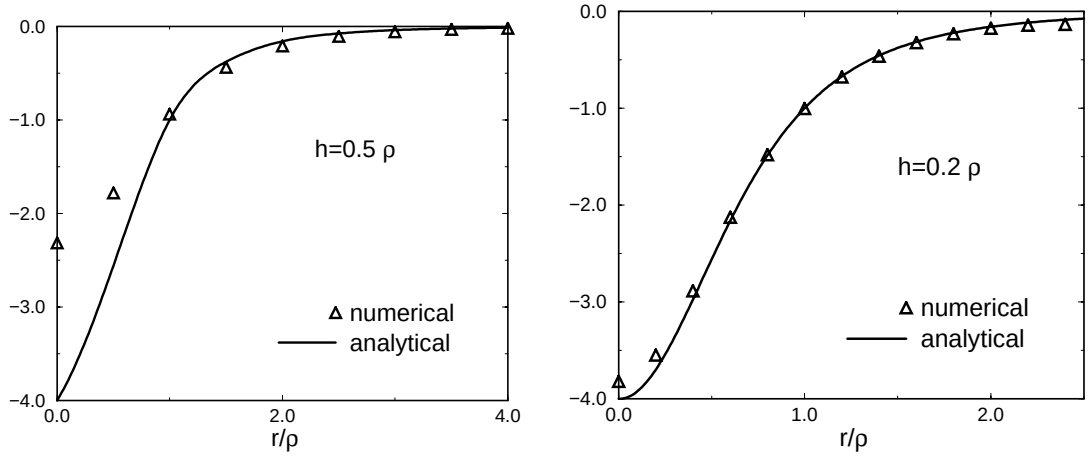

Fig. 3. The color-electric field $E_1^1(r = x_1)$ of an instanton for $x_{2,3,4} = 0$: The numerical solution (*triangles*) in comparison with the analytic result (6)

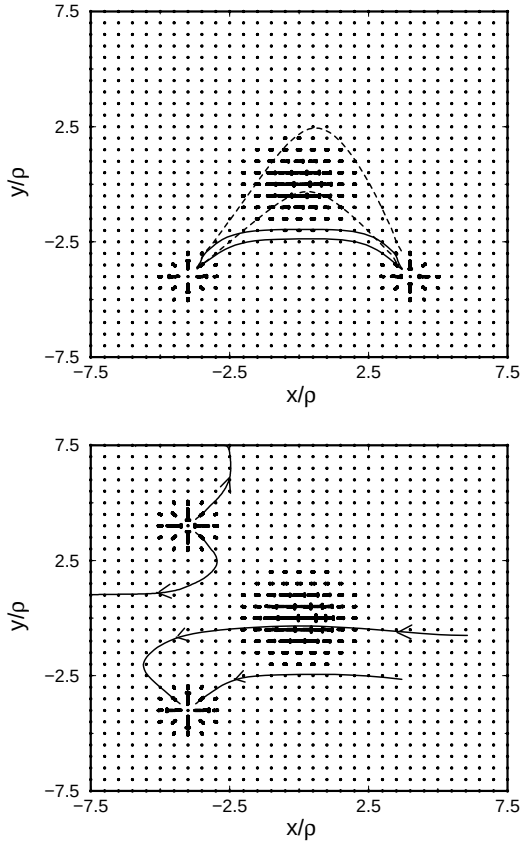

Fig. 4. The color-electric field $\mathbf{E}^1$ in the xy-plane produced by two color-electric charges in a state with one instanton present. The *dashed lines* indicate the field lines of the charges in an empty vacuum

ence of the boundaries becomes visible at the edges of the grid in the latter case.

4.3 Electric charges in empty space

In this subsection, we study the color-electric field produced by static color sources in non-Abelian SU(2) gauge theory. For this purpose, we have chosen the external current at the the r.h.s. of the equation of motion (4) to be

$$j_\mu^a(x) \;=\; \delta_{a1}\,\delta_{\mu 0}\;\left[\delta^{(3)}(\mathbf{x}-\mathbf{x}_1)\;-\;\delta^{(3)}(\mathbf{x}-\mathbf{x}_2)\right]\;. \quad (11)$$

This choice corresponds to two static color-electric charges of color direction $a = 1$ which are located at the spatial positions $\mathbf{x}_1$ and $\mathbf{x}_2$.

In order to get a feeling of the color-electric flux produced by these sources, we calculated the color-electric field $\mathbf{E}^{a=1}$ using an empty space as starting configuration of the iteration process, which solves the partial differential equation (4). To be specific, we have chosen

$$\mathbf{x}_1 \;=\; (4\rho, -4\rho, 0)\;, \qquad \mathbf{x}_2 \;=\; (-4\rho, -4\rho, 0)\;, \quad (12)$$

where ρ is an arbitrary length scale at the moment and will be the instanton radius later. If only sources for one color direction is present, the non-linear terms of the Yang-Mills equation of motion (4) drop out, and the e.o.m. essentially reduces to a Maxwell equation in the relevant color channel. For a later comparison with the case with an instanton present, we numerically calculated the color-electric field $\mathbf{E}^1$ in the xy-plane at each grid point. The color-electric field lines show the behavior anticipated from the analogy to classical electrodynamics.

4.4 Electric charges in the instanton background

The picture changes drastically, if the vacuum contains an instanton configuration. We here only consider sufficiently weak external charges which do not completely deform the instanton and which therefore preserve the pseudo-particle character of the instanton. In this limit, we are interested in the interplay of the color-electric field strengths of the

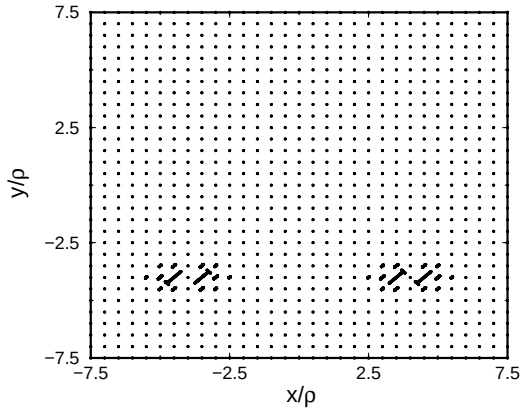

Fig. 5. The color-electric field $\mathbf{E}^1$ in the xy-plane of the charge instanton system with the color-electric field of the unperturbed instanton subtracted

external charges and the instanton as function of the collective coordinates. Note that in the presence of the external charges, the collective coordinates of an instanton in empty space do not correspond to zero-modes anymore, but a particular choice of these parameters exists, if the action is minimal. One possibility to constrain the collective coordinates is to include the term

$$\lambda \int d^4x \ \left(F^a_{\mu\nu}[A_{ex}] - F^a_{\mu\nu}[A]\right)^2 \qquad (13)$$

to the action. The field A_{ex} is thereby the gauge potential of a single instanton in empty space with a definite choice of origin, orientation and radius. The parameter λ acts like a Lagrange multiplier. For sufficiently small values of λ, the motion of the instanton along the (former) zero-mode directions due to the external source is blocked, and the collective coordinates are dictated by the background field. Using several (small) values of λ, one verifies that the field strengths configuration, produced by the instanton and the charges, remains (almost) unchanged by the additional term (13).

In order to be specific, the iteration process which minimizes the action was started with the analytic instanton configuration (6) (which is also used as the background field in (13)) casted onto the grid. The upper picture of Fig. 4 shows the result for $t = 0$, where the instanton develops its maximum strength. The color-electric field lines of the instanton, which point from the right to the left, are clearly visible. The length of the vectors on the grid points also give a rough impression of the instanton field strength profile (6). Some color-electric field lines are also shown (solid lines). For comparison, the color-electric field lines of the case without the instanton are shown as dashed lines, too. A field line is specified by the angle between the field line and the line connecting the two charges. This makes it possible to compare the situation with and without instanton. Our main observation is that the color-electric field lines of the charges are clearly expelled from the region where the instanton is located.

Let us study this effect, if the location of the two charges is changed to

$$\mathbf{x}_1 \ = \ (-4\rho, -4\rho, 0) \ , \qquad \mathbf{x}_2 \ = \ (-4\rho, 4\rho, 0) \ . \qquad (14)$$

The result is shown in the lower picture of Fig. 4. The upper charge is the source of the color-electric field, the lower charge is the drain. One observes that the color-electric field lines which spread out the upper charge are pushed back from the instanton, whereas the lines of the drain charge are pulled in. The net effect of the instanton is to align the external electric field lines with its internal orientation.

One might argue that the deformation of the color-electric field lines of the charges in the presence of the instanton is solely due to the superposition of the instanton field and the field from the charges. Figure 5 shows that this is not the case. In this picture, we have subtracted the color-electric field of a pure instanton (without any charges present) from the full color-electric field. If the total field is simply a superposition, one should recover the Maxwell type field lines (this is what would happen in classical electrodynamics). The result of this subtraction is completely different from the field distribution expected from classical electrodynamics. This is possible due to the non-linear nature of the classical equation of motion (4).

5 Random instanton orientation

In the previous section, we have investigated the distribution of the electric field strength, produced by a charge anti-charge pair, for a definite choice of the instanton orientation. No evidence for the dual Meissner effect was found so far, since the external color-electric field lines are attracted or pulled back from the instanton core depending on the orientation. Here, we will study whether a net repulsion of the color-electric field lines takes place, if the we average over the instanton orientation. For this purpose, we will calculate the space-time distribution the field strength squared $F^a_{\mu\nu}F^a_{\mu\nu}$, where we average over the orientation of the instanton and keep its position fixed. The case of the random instanton orientation is interesting from a physical point of view for the following reason: a realistic description of the Yang-Mills ground state resorts to a liquid of instantons [15]. In this liquid, the orientation of a particular instanton is arbitrary. The small amounts of action which are necessary to move the instanton along its former (i.e. single instanton) zero-mode directions are provided by the entropy of the medium.

Let us first study the dependence of the instanton interaction with the external charges on the orientation O^{ab} of the instanton, i.e.

$$A^{a\,inst}_\mu(x) \ = \ O^{ab}\eta^b_{\mu\nu}x_\nu \, \frac{2}{x^2+\rho^2} \ ,$$
$$O \ = \ \begin{pmatrix} \cos\theta & -\sin\theta & 0 \\ \sin\theta & \cos\theta & 0 \\ 0 & 0 & 1 \end{pmatrix} \ , \qquad (15)$$

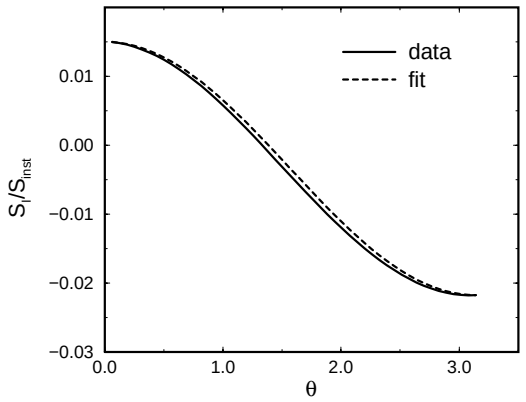

Fig. 6. The instanton interaction S_I as function of the instanton orientation θ

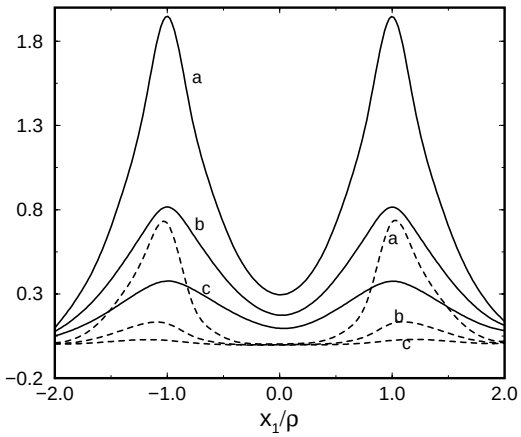

Fig. 7. $(F^a_{\mu\nu}F^a_{\mu\nu})^{1/2}(x_1, x_2, x_{0,3} = 0)$ for several values of x_2 (cases a-c) of the charges in empty space (*solid*) and of the instanton-charge system with $(F^2)^{1/2}$ of an unperturbed instanton subtracted (*dashed*). In the case of the instanton-charge system, we have averaged over the instanton orientations

where O^{ab} is a particular orthogonal matrix parameterized by the angle θ. Since we will switch on electric charges in color $a = 1$ direction, it is sufficient for our purposes to study matrices O^{ab} which rotate the instanton color-electric field in the x_1x_2-plane only. The instanton interaction S_I is defined by

$$S_I \;=\; S_{IC} \,-\, S_{inst} \,-\, S_{charges}\;, \qquad (16)$$

where S_{IC} is the action of the instanton-charge system, and S_{inst} and $S_{charges}$ is the action of a single instanton and the charges, respectively. If the charges are weak and far located from the instanton origin, the interaction S_I can be calculated in an elegant way [16], i.e.

$$S_I^0 \;\propto\; \eta^a_{\mu\nu} F^{a\,ext.}_{\mu\nu}\;, \qquad (17)$$

where $F^{a\,ext.}_{\mu\nu}$ is the field strength of the external charges at the instanton origin, and where the superscript indicates that it was assumed that the this field strength is slowly varying over the instanton region. If we align the charges in $\hat{e}_1$-direction symmetric to the x_2-axis, their color-electric field at the instanton center is also oriented in $\hat{e}_1$ direction. This implies that $S_I^0 \propto \cos\theta$ for the particular choice of orientation (15). The numerical result for S_I is shown in Fig. 6. The strengths of the charges actually yield $S_{charges}/S_{inst} = 6.7\%$. The distance of one charge to the instanton center was $1.7\,\rho$. A fit according $S_I \approx a\,\cos\theta + b$ is also shown in Fig. 6. A $\cos\theta$-modulation of the data, as predicted by (17), is clearly visible. In addition, one observes a non-vanishing offset b towards negative values. This offset can be understood as follows: if we put the field configurations of the charges and of the unperturbed instanton on the grid as starting configuration, the method of steepest decent further reduces the action in order to finally arrive at a solution of the Yang-Mills equations of motion. Since action of the starting configuration does not depend of the instanton orientation, the angle average of S_I is negative. From this argument, it is obvious that the offset b cannot obtained in the linear response approach, which is the basis of (17).

Finally, we will average over the θ-angle, which defines the instanton orientation with respect to the charges. We will study the variation of the field strength squared, i.e. $F^a_{\mu\nu}F^a_{\mu\nu}(x)$, in space-time rather than the integrated quantity S_I. Since F^2 of a single instanton decreases like $1/r^8$ for large distances r from the instanton center and since F^2 of a single charge asymptotically behaves like $1/r^4$, it is more convenient for illustration purposes to study the quantity $\sqrt{F^2}$. In the present investigation, we have located the charges at

$$\mathbf{x}_1 \;=\; (\rho, -\rho, 0)\;, \qquad \mathbf{x}_2 \;=\; (-\rho, -\rho, 0)\;, \qquad (18)$$

Figure 7 shows $\sqrt{F^2}$ of the charge anti-charge pair (solid lines) as function of x_1 ($x_{3,0} = 0$) for several values of x_2, i.e. case a $x_2 = -0.4\,\rho$, case b $x_2 = -0.2\,\rho$ and case c $x_2 = 0$. This result is compared with $\sqrt{F^2}_{cI}$ produced by the instanton charge configuration (dashed lines), where $\sqrt{F^2}$ of a single instanton was subtracted and where over the orientations of the instanton was averaged. The latter quantity is therefore a measure of the field strength which exists on top of that of an unperturbed instanton. One clearly observes that $\sqrt{F^2}$ produced by the external charges is suppressed at the space time region occupied by the instanton. In order to quantify this result, we introduce the ratio

$$\kappa(x_2) \;=\; \frac{\left[\sqrt{F^2}^{\,peak}_{charges}(x_2) \,-\, \sqrt{F^2}^{\,peak}_{cI}(x_2)\right]}{\sqrt{F^2}^{\,peak}_{charges}(x_2)}\;, \qquad (19)$$

where $\sqrt{F^2}^{\,peak}_{charges}$ and $\sqrt{F^2}^{\,peak}_{cI}$ are the maximum values of $\sqrt{F^2}$ of the charges in empty space and of the subtracted charge instanton system, respectively, at a given line $(x_2, x_{3,0} = 0)$. The ratio κ directly measures the suppression of the external color-electric field inside the instanton. The numerical calculation reveals the following result

x_2	0	-0.2	-0.4	-0.6
κ	92%	84%	63%	28%

One finds that a net suppression of the external field inside the instanton occurs, if over the instanton orientation is averaged. The suppression increases towards the instanton center.

6 Discussions and conclusions

Among many other things, Polikarpov and Veselov studied the instanton medium which emerges in lattice Yang-Mills theory, if an equilibrium configuration is cooled down [27]. They found in particular, that this cooled medium exhibits a non-vanishing string tension, which, however, is only 5% of the full string tension. Whether this residual confinement is due to some excitations still present on top of the instantons at the cooled lattice or due to an intrinsic property of the instanton medium is not clear yet.

In order to provide new information concerning the interesting question whether the instantons play a role for the dual Meissner effect, we have studied the impact of an instanton on the color-electric flux produced by two static, point-like color-electric charges. The classical equation of motion of a SU(2) gauge theory was numerically solved in Lorentz gauge. The color-electric field lines of the charges were investigated in detail in an "empty" vacuum as well as in a state where an instanton is present. We found that the external color electric field lines are expelled or attracted depending on the orientation of the instanton relative to the charges. The net effect is that the instanton aligns the external field lines which is in accordance with the result of the leading order of the linear response theory [16]. However, if we average over the orientations of the instanton, this leading order effect drops out. In subleading order, a substantial repulsion of the color-electric field lines from the instanton core region survives.

The numerical outcome can be qualitatively understood as follows: in an "empty" space, the electric flux spreading out the charges distributes over the whole space in order to avoid large concentrations of field strength which amounts for a large action. If only charges of unique color are present, the scenario is the same for the Abelian (classical electro-dynamics) and the non-Abelian case. However, the non-linearity of the Yang-Mills equation of motion (in fact the topological structure of the theory) allows for non-trivial configurations, i.e. instantons, which are local minima of the Yang-Mills action. These configuration must exhibit a definite strength of the color-electric and color-magnetic field (see (6)) in order to minimize the action. Any distortion of the instanton field strength, e.g. produced by the presence of external charges, yields a sudden increase of the action. This is the reason that the color-electric field is expelled from the instanton core region, once the dominant dipole interaction of the instanton with the charges drops out due to a random instanton orientation.

Whether this effect is a pre-cursor of quark confinement giving rise to a non-vanishing string tension, if the Yang-Mills ground state is modeled as a strongly correlated medium of randomly oriented instantons, is an interesting question, which is left to future studies.

Acknowledgements. I thank E. V. Shuryak for useful informations and interesting comments, and Mannque Rho for helpful remarks. I am also indebted to H. Reinhardt for many discussions on the issue of monopole condensation in Yang-Mills theories as well as support.

Appendix: Euclidean gauge theory

The Euclidean partition function of a SU(2) gauge theory, fermions included, is described by the functional integral

$$Z = \int \mathcal{D}q\, \mathcal{D}q^\dagger\, \mathcal{D}A^a_\mu\, \exp\left\{ - \int d^4x \right. \\ \left. \times \left[\frac{1}{4g^2} F^a_{\mu\nu} F^a_{\mu\nu} + q^\dagger (i\partial\!\!\!/ + im - A^a_\mu t^a) q \right] \right\} \, , \quad (20)$$

where the gauge fields A^a_μ are considered as real fields, and where the fermion fields q transform under the fundamental representation of the $SU(2)$ gauge group which is spanned by the generators t^a. g is the gauge coupling constant and m is current quark mass. The action is invariant, if the fields transform under a global O(4) symmetry, i.e.

$$A^{a\,\prime}_\mu \;=\; \Lambda_{\mu\nu} A^a_\nu \, , \qquad q' \;=\; S(\Lambda) q \, , \quad (21)$$

which is the pendant to the Lorentz symmetry in Minkowski space. The orthogonal matrices $\Lambda_{\mu\nu}$ and the matrices $S(\Lambda)$ are spanned by the anti-symmetric generators $\omega_{\mu\nu}$, e.g. $\Lambda_{\mu\nu} \;=\; [\exp\{-\omega\}]_{\mu\nu}$. The matrices $S(\Lambda)$ satisfy

$$S(\Lambda) \gamma_\mu S^\dagger(\Lambda) \;=\; \Lambda_{\mu\nu} \gamma_\nu \, , \quad (22)$$

where γ_μ are the hermitian Dirac matrices which fulfill $\{\gamma_\mu, \gamma_\nu\} = 2\delta_{\mu\nu}$. From (22), it is obvious that

$$j^a_\mu(x) \;=\; q^\dagger(x)\, \gamma_\mu\, t^a\, q(x) \quad (23)$$

is a hermitian current which transforms like a O(4) vector. The zeroth component of this vector is the charge density which is the subject of investigations in this paper.

Finally, let us check that the coupling of the current (5) to the gauge fields A^a_μ is correctly chosen, i.e. a gauge transformation does not induce imaginary parts in A^a_μ. One easily observes that the transformation

$$q'(x) \;=\; U(x) q(x) \, , \qquad U(x) \in SU(2) \quad (24)$$

leaves the action invariant, if the gauge fields transform according

$$t^a A^{a\,\prime}_\mu(x) \;=\; U(x)\, t^a A^a_\mu(x)\, U^\dagger(x) - i U(x) \partial_\mu U^\dagger(x) \, . \quad (25)$$

It is easy to verify that the transformation (25) leaves the gauge field A^a_μ real. The contribution of the interaction of the quark current and the gauge fields to the Euclidean action is therefore

$$S_{int} \;=\; - \int d^4x\; j^a_\mu(x) A^a_\mu(x) \, . \quad (26)$$

It is straightforward to derive the equation of motion (4) from the action in (20) by taking the functional derivative with respect to the gauge fields $A^a_\nu(x)$.

We here provide the right hand side of the equation of motion (4), i.e. the current, and calculate the gauge fields. First information on the gauge fields can be obtained by taking the divergence of the equation of motion. Using the e.o.m., a direct calculation yields

$$\partial_\nu j^a_\nu(x) \;=\; \epsilon^{abc} A^b_\mu(x) j^c_\mu(x)\;. \qquad (27)$$

In this paper, we study the response of the gauge fields to static charges, i.e.

$$j^a_\mu(x) \;=\; \delta_{\mu 0} \sum_i \rho^a_i\, \delta(\mathbf{x}-\mathbf{x_i})\;. \qquad (28)$$

Equation (27) then tells us that the zeroth component of the gauge fields at the position of the charges either vanishes, i.e. $A^a_0(t,\mathbf{x_i}) = 0$, or that the gauge fields are oriented parallel to the charge color vector, i.e. $A^a_0(t,\mathbf{x_i}) \propto \rho^a_i$.

References

1. K. G. Wilson, Phys. Rev. **D10** (1974) 2445; M. Creutz, Phys. Rev. **D21** (1980) 2308; Phys. Rev. Lett. **45** (1980) 313; G. Münster, Phys. Lett. **B95** (1980) 59; C. Rebbi, *Lattice gauge theories and Monte Carlo simulations* (World Scientific Publishing, Singapore, 1983)
2. J. Engels, J. Jersak, K. Kanaya, E. Laermann, C. B. Lang, T. Neuhaus, H. Satz, Nucl. Phys. **B280** (1987) 577. A. D. Giacomo, M. Maggiore, S. Olejnik, Nucl. Phys. **B347** (1990) 441. L. D. Debbio, A. D. Giacomo, Phys. Lett. **B267** (1991) 254. T. L. Ivanenko, A. V. Pochinskii, M. I. Polikarpov, Phys. Lett. **B302** (1993) 458
3. *see e.g* M. Jaminon, R. M. Galain, G. Ripka and P. Stassart, Nucl. Phys. **A537** (1992) 418; H. Weigel, R. Alkofer and H. Reinhardt, Phys. Rev. **D49** (1994) 5958
4. C. D. Roberts, A. G. Williams, Prog. Part. Nucl. Phys. **33** (1994) 477-575; L. v. Smekal, P. A. Amundsen, R. Alkofer, Nucl. Phys. **A529** (1991) 633
5. K. Langfeld, M. Rho, Nucl. Phys. **A596** (1996) 451; K. Langfeld, Nucl. Phys. **A602** (1996) 375
6. G. 't Hooft, *High energy physics*, Bologna **1976**; S. Mandelstam, Phys. Rep. **C23** (1976) 245; G. 't Hooft, Nucl. Phys. **B190** (1981) 455
7. *see e.g* A. S. Kronfeld, G. Schierholz, U.-J. Wiese, Nucl. Phys. **B293** (1987) 461
8. T. Banks, M. Spiegelglas, Nucl. Phys. **B152** (1979) 478; V. P. Nair, C. Rosenzweig, Phys. Rev. **D31** (1985) 401
9. N. Seiberg and E. Witten, Nucl. Phys. **B426** (1994) 19; Nucl. Phys. **B431** (1994) 484
10. A. M. Polyakov, Phys. Lett. **B59** (1975) 82; A. A. Belavin, A. M. Polyakov, A. A. Schwartz, Yu. S. Tyupkin, Phys. Lett. **B59** (1975) 85; A. A. Belavin, A. M. Polyakov, JETP Lett **22** (1975) 245; G. t'Hooft, Phys. Rev. Lett. **37** (1976) 8
11. M. F. Atiyah, R. S. Ward, Comm. Math. Phys. **55** (1977) 177; M. F. Atiyah, N. J. Hitchin, V. G. Drinfeld, Yu. I. Manin, Phys. Lett. **A65** (1978) 185
12. H. Reinhardt, K. Langfeld, Phys. Lett. **B317** (1993) 590
13. for a recent review see e.g. D. Diakonov, hep-ph/9602375
14. G. 't Hooft, Phys. Rev. Lett. **37** (1976) 8; Phys. Rev. **D14** (1976) 3432
15. E. V. Shuryak, Nucl. Phys. **B203** (1982) 93; Nucl. Phys. **B302** (1988) 259; D. I. Dyakonov, V. Yu. Petrov, Phys. Lett. **B130** (1983) 385, Nucl. Phys. **B245** (1984) 259; E. V. Shuryak, J. J. M. Verbaarschot, Nucl. Phys. **B341** (1990) 1
16. C. G. Callan, R. Dashen, D. J. Gross, Phys. Rev. **D17** (1978) 2717; Phys. Rev. **D19** (1978) 1826
17. K. Langfeld, H. Reinhardt, Phys. Lett. **B333** (1994) 396
18. M. Schaden, H. Reinhardt, P. A. Amundsen, M. J. Lavelle, Nucl. Phys. **B339** (1990) 595; P. A. Amundsen, M. Schaden, Phys. Lett. **B252** (1990) 265
19. K. Langfeld, H. Reinhardt, Nucl. Phys. **A579** (1994) 472
20. M. N. Chernodub, F. V. Gubarev, JETP Lett. **62** (1995) 100; H. Suganuma, K. Itakura, H. Toki, O. Miyamura, *Correlations between instantons and monopoles in the abelian gauge*, hep-ph/9512347
21. R. C. Brower, K. N. Orginos, C.-I Tan, hep-lat/9608012, hep-th/9610101
22. A. Hart, M. Teper, Phys. Lett. **B371** (1996) 261; B. Alles, M. D'Elia, A. Di Giacomo, *Topological suszeptibility at zero and finite T in SU(3) Yang-Mills theory*, hep-lat/9605013
23. H. Markum, W. Sakuler, S. Thurner, Symposium on Lattice Field Theory, Melbourne, proceedings Lattice **1995**
24. M. Feurstein, H. Markum, S. Thurner, *Instantons and Monopoles in Lattice QCD*, hep-lat/9702006; *Coexistence of monopoles and instantons for different topological charge definitions and lattice actions*, hep-lat/9702004
25. Y. Aharonov, A. Casher, S. Yankielowicz, Ncul. Phys. **B146** (1978) 256
26. E. V. Shuryak, Phys. Lett. **B79** (1978) 135
27. M. I. Polikarpov, A. I. Veselov, Nucl. Phys. **B297** (1988) 34
28. W. Buerger, M. Faber, H. Markum, M. Müller, M. Schaler, Dallas 1993, Proceedings, Lattice93, Nucl. Phys. **B34** (1994) 269, Proc. Suppl
29. N. W. Ashcroft, N. D. Mermin, *Solid State Physics*, Holt-Saunders International Edition 1981
30. V. L. Gizburg, L. D. Landau, Zh. Eksp. Teor. Fiz. **20** (1950) 1064